Looking for Signs of the Pomeron

Toward Mueller-Tang Jets at Next-to-Leading Order

Timothy Raben
timothy.raben@ku.edu

International Symposium on Multiparticle Dynamics : Tlaxcala, Tlaxcala, Mexico 2017

BROWN

Stanford
University

U.PORTO

Outline

- Introduction to Pomeron Physics
- Previous Application of Regge Physics
- Pomerons in Future Jet Processes
- Conclusions & Future

Regge theory and the Pomeron

Regge Theory grew out of pre-QCD S-matrix theory of the 50's and 60's. Amplitudes are seen as unitary, Lorentz invariant functions of analytic momenta. (doesn't assume an underlying theory) Amplitudes have poles representing particle exchange. Using a partial wave analysis, dominant contribution to simple amplitudes is the exchange of an *entire trajectory* of particles: Pomeron exchange: $\sigma_{tot} \sim s^{\alpha_0} - 1$

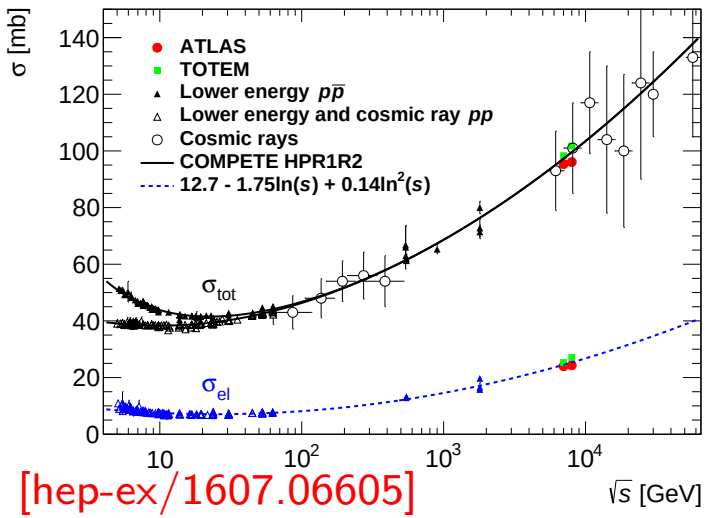

[hep-ex/1607.06605]

This soft Pomeron has been used to fit to p-p total cross sections since '70s.

Authors	$\alpha_{\mathcal{P}}(0)$
Donnachie-Landshoff (1992)	1.0808
Cudell, Kang and Kim (1997)	$1.096^{+0.012}_{-0.009}$
Cudell *et al.* (2000)	1.093 ± 0.003
COMPETE Collaboration (2002)	1.0959 ± 0.0021
Luna and Menon (2003)	1.085 - 1.104
Menon and Silva (2013)	1.0926 ± 0.0016

Throughout this talk I will mainly be focused on single Reggeon exchange although I might comment on the end about multi-Reggon exchange, Regge cuts, and saturation

BFKL

Balitsky, Fadin, Kuraev, Lipatov (BFKL): perturbative Pomeron. Large logs get in the way of usual perturabtion theory: resum $\alpha_s\, log(s)$ to all orders. Bfkl equation – integral equation for Green's function in Mellin space

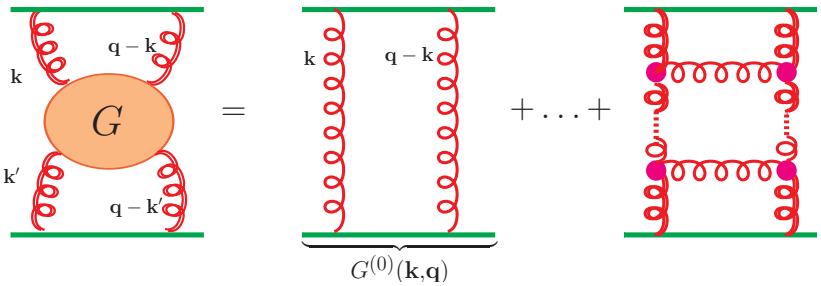

$$G(\mathbf{k},\mathbf{k}',\mathbf{q},Y) = \int_{-i\infty}^{+i\infty} \frac{d\omega}{2\pi i} e^{Y\omega} f_\omega(\mathbf{k},\mathbf{k}',\mathbf{q}) \to \int_{-i\infty}^{+i\infty} \frac{d\omega}{2\pi i} e^{Y\omega} \sum_{n\in\mathcal{Z}} \int_{\frac{1}{2}-i\infty}^{\frac{1}{2}+i\infty} \frac{d\gamma}{2\pi\, i} \frac{E_{\gamma,n}(k) E^*_{\gamma,n}(k')}{\omega - \bar{\alpha}_s \chi(\gamma,n)}$$

where in Leading Log (LL)

$$\chi(\gamma,n) = 2\psi(1) - \psi(\gamma + \frac{|n|}{2}) - \psi(1-\gamma+\frac{|n|}{2}) \quad \textit{and} \quad \omega_0 = \frac{4\alpha_s N_c}{\pi} ln(2)$$

Surprising conformal symmetry greatly simplifies things in coordinate space

Holographic(BPST) Pomeron

AdS/CFT: identify the Pomeron: **the Regge trajectory of the graviton** [hep-th/0603115]Scattering amplitudes computed via Feynman diagram like approach [hep-th/9802150] with the leading Regge amplitudes:

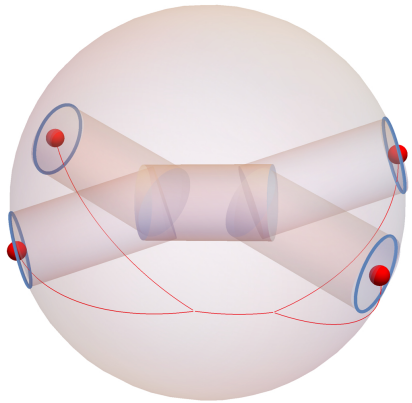

$$\psi_1(z)\psi_2(z) * \chi(z,z',s,t) * \psi_3(z')\psi_4(z')$$

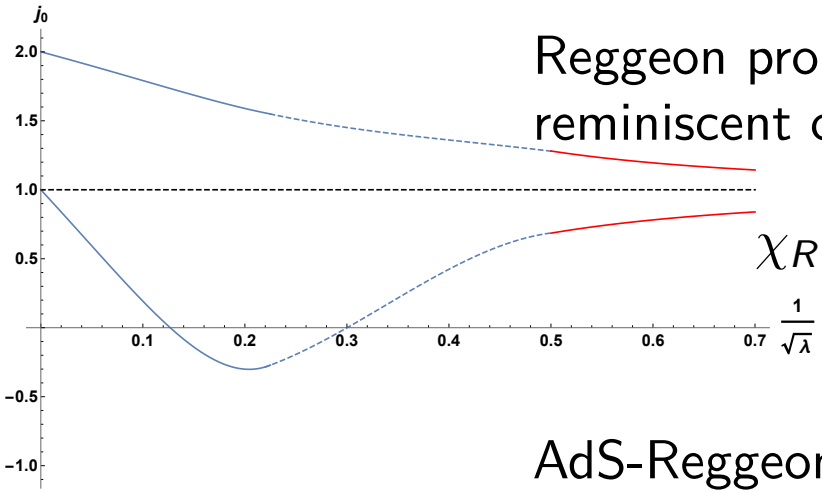

Reggeon propagators
reminiscent of the weak coupling partonic description

$$\chi_R \sim \int dj(\alpha'\hat{s})^j(1+Cos(-i\pi j))G_j(t,z,z')$$

AdS-Reggeons: operator dimensions have an anomalous part and admit a non-trivial convergent expansion in terms of spin, coupling, and twist. These $\Delta - J$ curves can be calculated to high order using a mix of conformal, string, and integrability techniques. Minimizing these curves gives Reggeon intercepts. [hep-th/1409.2730]

Applications of BPST-Pomeron

Total cross section for deep inelastic scattering. Focus on small-x data coming from combined ZEUS+H1 experiments at HERA. [hep-ph/1007.2259, hep-ph/1412.3443, hep-ph/1508.05063]

Model	ρ	g_0^2	z_0	Q'	χ^2_{dof}
conformal	0.774*	110.13*	–	0.5575*GeV	11.7 (0.75*)
hard wall	0.7792	103.14	4.96 GeV^{-1}	0.4333 GeV	1.07 (0.69*)
softwall	0.7774	108.3616	8.1798 GeV^{-1}	0.4014 GeV	1.1035
softwall*	0.6741	154.6671	8.3271 GeV^{-1}	0.4467 GeV	1.1245

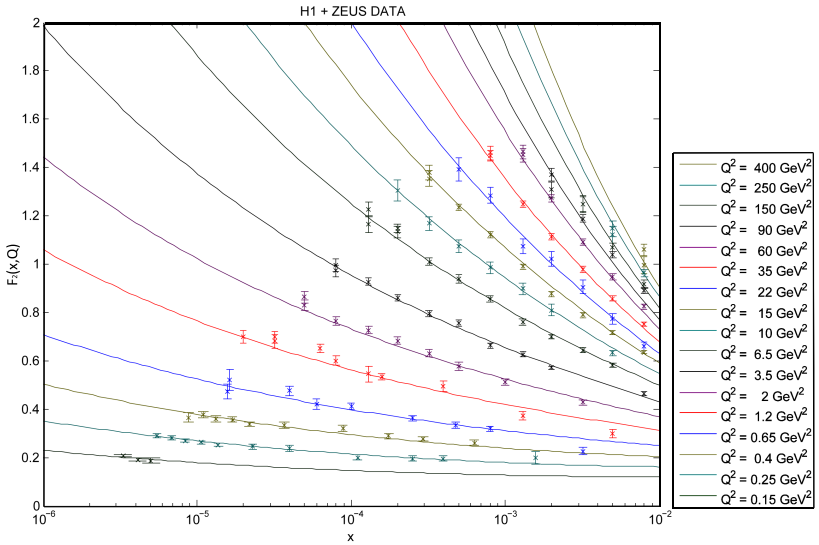

(all statistical errors $\sim 1\%$)

$$F_2(x, Q^2) = \frac{Q^2}{4\pi^2\alpha_{em}}\sigma_{tot} \sim \frac{Q^2}{s4\pi^2\alpha_{em}} Im[\chi(s, t = 0)]$$

Similar types of studies have been done for vector meson production [hep-ph/1307.0009], diffractive Higgs production [hep-ph/1202.4953], to predict glueball masses [hep-ph/1508.00008], cross sections of non-diffractive central η production [hep-ph/1612.07457], and others.

Applications of BPST-Pomeron II

Differential cross section for inclusive central production computed via Mueller's generalized optical theorem applied to Regge scattering in AdS/CFT.

$$\frac{1}{\sigma_{tot}}\frac{d^3\sigma_{ab\to X}}{d\boldsymbol{p}_\perp^2\, dy} \sim \frac{1}{2i\,s} Disc_{M^2>0}[\mathcal{T}_{abc'\to a'b'c}] \sim \frac{A}{(\boldsymbol{p}_\perp + C)^B}$$

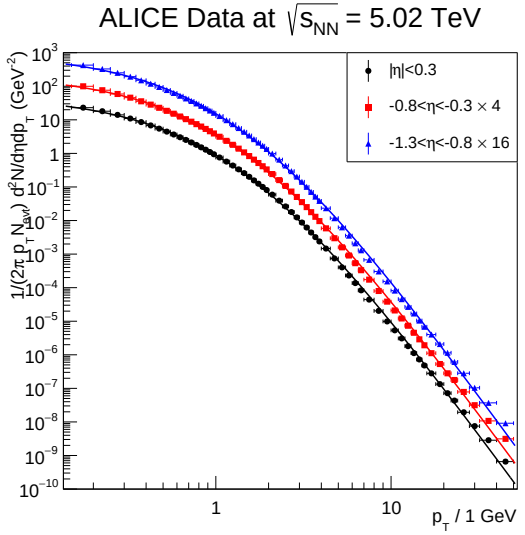

Focus on p-pb ALICE $\sqrt{s_{NN}}$=5.02 TeV, p-p ATLAS 8 TeV, and 13 TeV data sets. [hep-ph/1702.05502]

Dataset	A/10 (GeV^{-2})	B	C/(1 GeV)
ALICE 5.02 TeV, $\|\eta\| < 0.3$	38.48 ± 8.26	7.23 ± 0.09	1.32 ± 0.04
ALICE 5.02 TeV, $-0.8 < \eta < -0.3$	37.60 ± 7.97	7.22 ± 0.08	1.30 ± 0.04
ALICE 5.02 TeV, $-1.3 < \eta < -0.8$	43.00 ± 9.29	7.30 ± 0.09	1.31 ± 0.04
ATLAS 8 TeV	4.46 ± 2.60	7.03 ± 0.264	1.07 ± 0.123
ATLAS 13 TeV	5.77 ± 3.38	6.96 ± 0.265	1.12 ± 0.126

Results show conformal behavior near $B = 2\Delta = 8$ regardless of confinement model used.

Mueller-Navelet Jets

Mueller Navelet jets
can be described via BFKL framework. Important observable is the decorrelation of azimuthal jet angles for jets widely separated by rapidity

- LL BFKL overestimates this effect
- LL BFKL
  + running coupling + DGLAP does a decent job (How to disentangle BFKL effects?)
- Full NLL BFKL including NLO vertices and colinear resummation [hep-ph/1002.1365]similar or not as good as NLO-DGLAP

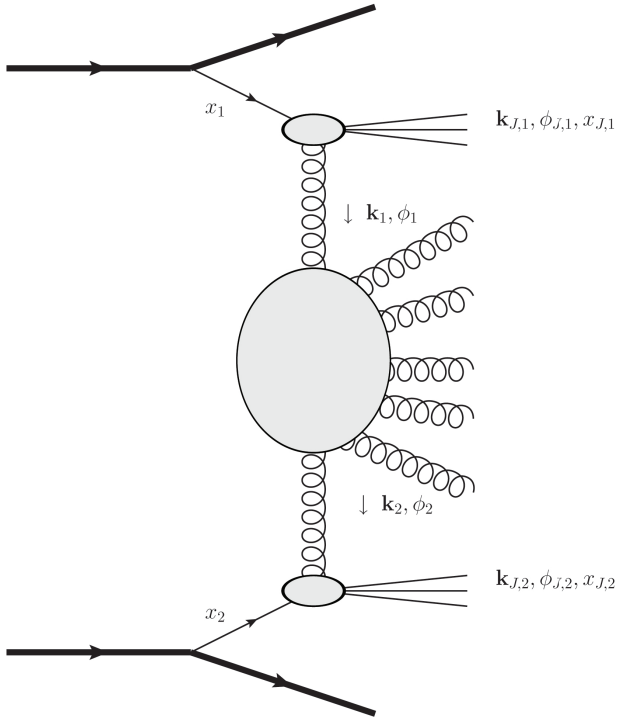

[hep-ph/1002.1365]

$$\frac{d\sigma}{dy_1 dy_2 d|k_1^{\perp}| d|k_2^{\perp}| d\phi_1 d\phi_2} = \frac{1}{(2\pi)^2} \sum_{n=0}^{\infty} 2cos(n\phi) C_n$$

Mini jets?

What about other observables? [hep-ph/1610.01334] BFKLex

$$\langle p_T \rangle = \frac{1}{N}\sum_{i=1}^{N} |p_{Ti}| \quad \langle \phi \rangle = \frac{1}{N}\sum_{i=1}^{N} \phi_i \quad \langle R_y \rangle = \frac{1}{N+1}\sum_{i=1}^{N+1} \frac{y_i}{y_{i-1}}$$

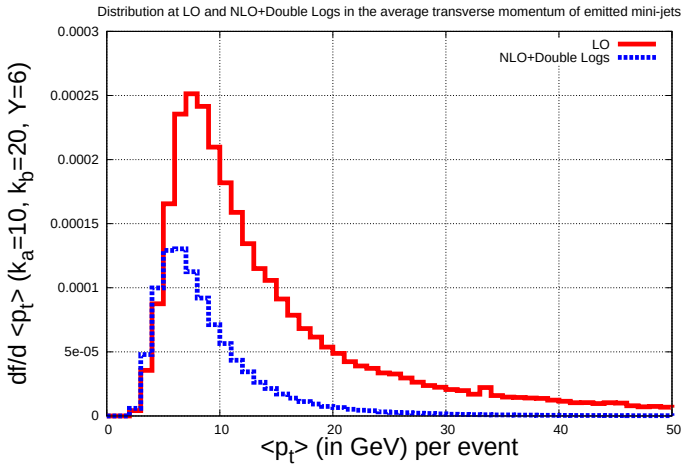

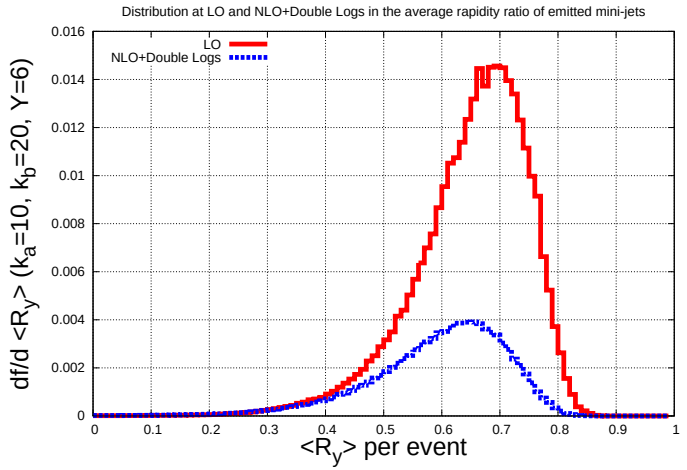

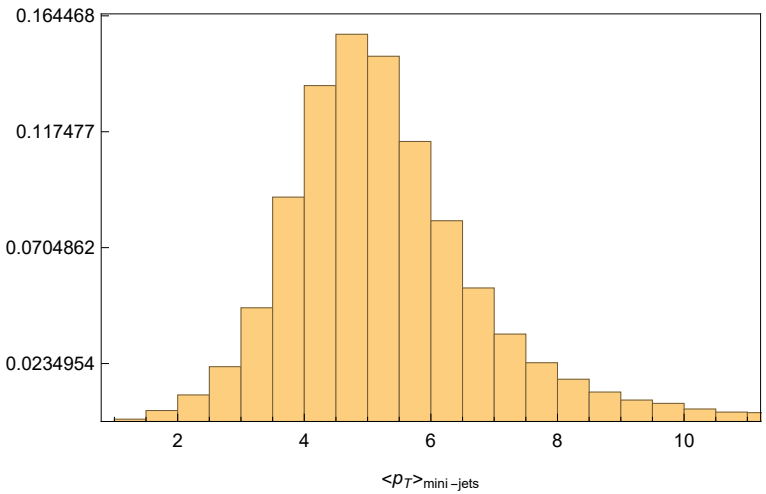

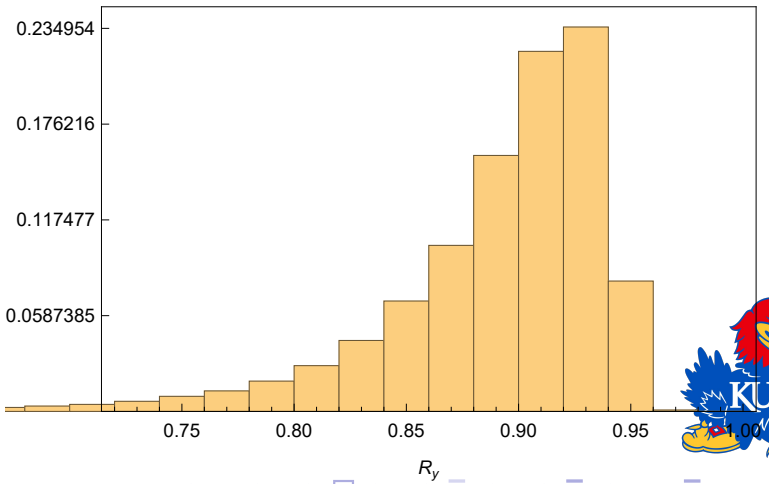

Mueller Tang: Jet gap jet

Using rapidity gaps to investigate BFKL effects dates back to early '90s [Phys. Rev. D 47 1 (1993)] Mueller and Tang: augmented BFKL hard Pomeron.

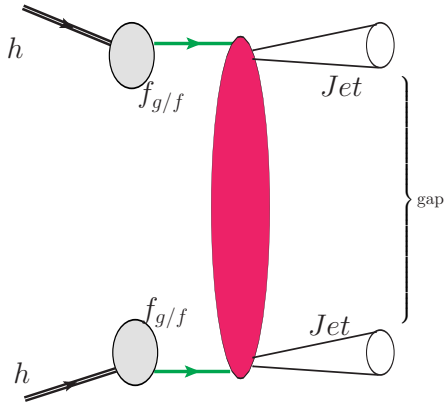

$$E_{n\nu}(\rho_1,\rho_2) = \underbrace{\left(\frac{\rho_1-\rho_2}{\rho_1\rho_2}\right)^h\left(\frac{\rho_1^*-\rho_2^*}{\rho_1^*\rho_2^*}\right)^{\bar{h}}}_{\text{Lipatov term}} \underbrace{-\left(\frac{1}{\rho_2}\right)^h\left(\frac{1}{\rho_2^*}\right)^{\bar{h}}-\left(\frac{-1}{\rho_1}\right)^h\left(\frac{-1}{\rho_1^*}\right)^{\bar{h}}}_{\text{Mueller-Tang correction}}$$

At finite momentum transferred can be investigated at hadron colliders looking for highly exclusive processes where two jets far apart in rapidity represent the sole observed radiation. The absence of any additional emission over a large rapidity region suggests that the color-singlet exchange contributes substantially to the jet-gap-jet cross section.

DGLAP suppressed at large Δy $\rightarrow$ Good window into BFKL effects.

previous fits and analysis

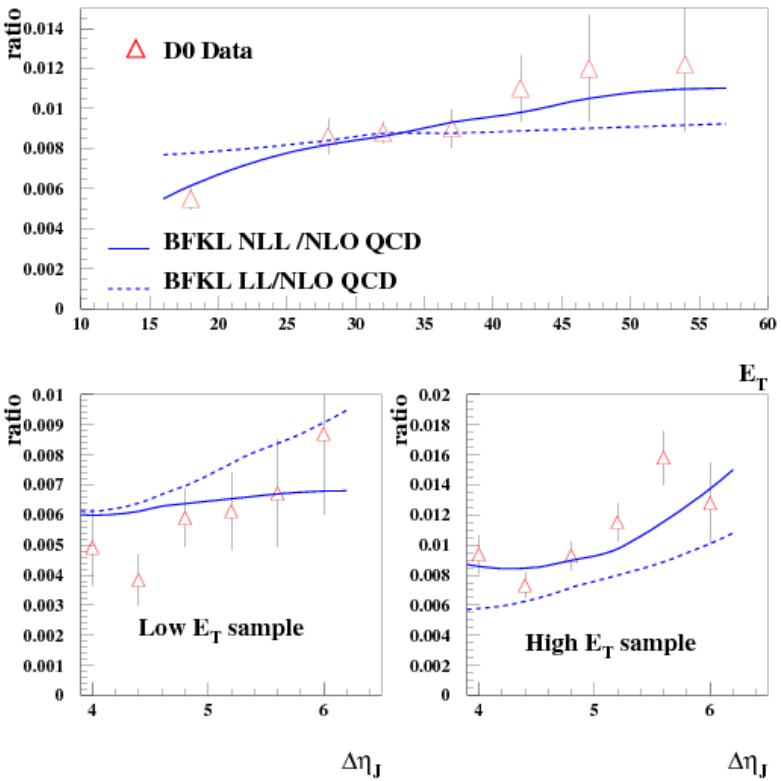

Left: LL & NLL BFKL at Tevatron [hep-ph/1012.3849].

Right LL+SCI at CMS [hep-ph/1703.10919].

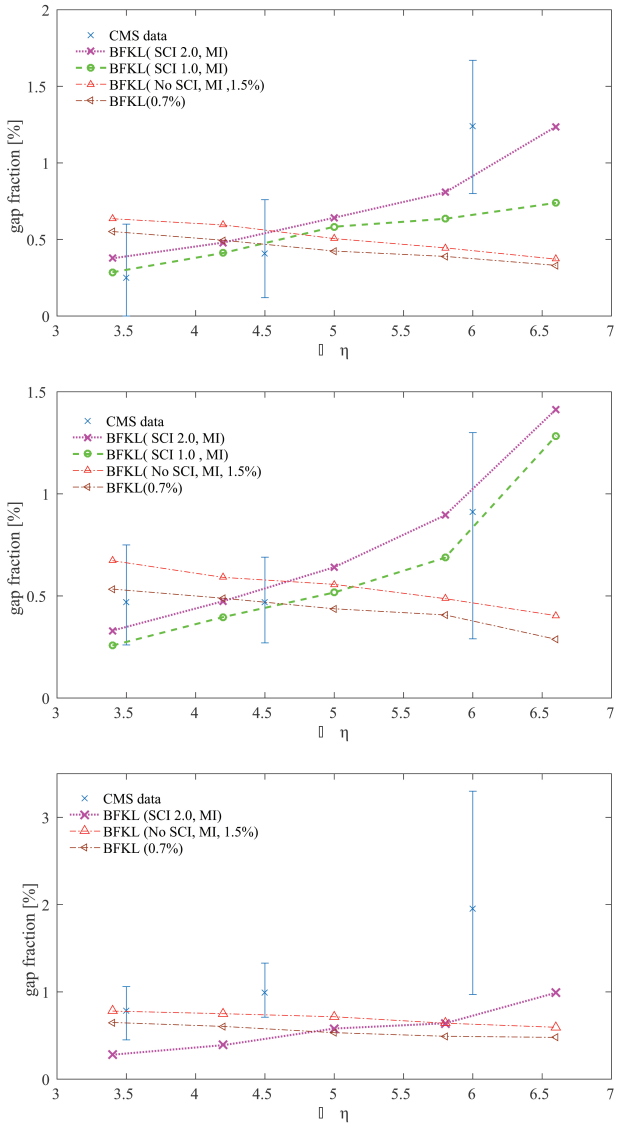

incorporating NLO impact factor

A full NLL/O calculation is within reach. NLO MT impact factors recently calculated [1406.5625,1409.6704]. Very complicated! (not in a factorizable form!) But...only certain combinations of jet vertex and Green's function approximation orders contribute effectively to the NL order of the cross section. The most complicated combinations can be discarded because they are subleading.

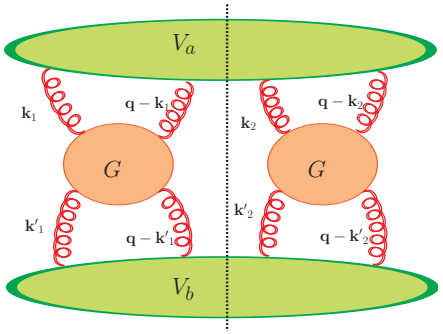

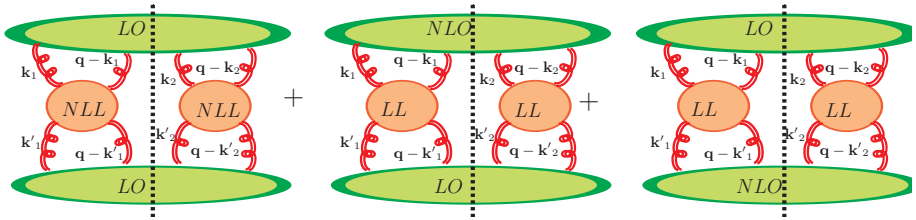

- GGF NLL + LO vertices. For this special case the general formula for the cross section can be expressed in a much simpler form because LL vertices are idependent from the reggeon momenta.
- GGF LL + LO vertex + NLO vertex. The non trivial dependence of the NLO jet vertex from the reggeon momenta introduces an important complication.
- GGF LL + both NLO vertices. Discarded because subleading.

details of NLO impact factor

details of NLO impact factor

$$\frac{d\hat{V}^{(1)}(x,\boldsymbol{k},\boldsymbol{l}_1,\boldsymbol{l}_2;x_J,\boldsymbol{k}_J;M_{X,\max},s_0)}{dJ} =$$

$$= v_q^{(0)}\frac{\alpha_s}{2\pi}\left[S_J^{(2)}(\boldsymbol{k},x)\cdot\left[-\frac{\beta_0}{4}\left[\left\{\ln\left(\frac{\boldsymbol{l}_1^2}{\mu^2}\right)+\ln\left(\frac{(\boldsymbol{l}_1-\boldsymbol{k})^2}{\mu^2}\right)+\{1\leftrightarrow 2\}\right\}-\frac{20}{3}\right]-8C_f\right.$$

$$+\frac{C_a}{2}\left[\left\{\frac{3}{2\boldsymbol{k}^2}\left\{\boldsymbol{l}_1^2\ln\left(\frac{(\boldsymbol{l}_1-\boldsymbol{k})^2}{\boldsymbol{l}_1^2}\right)+(\boldsymbol{l}_1-\boldsymbol{k})^2\ln\left(\frac{\boldsymbol{l}_1^2}{(\boldsymbol{l}_1-\boldsymbol{k})^2}\right)-4|\boldsymbol{l}_1||\boldsymbol{l}_1-\boldsymbol{k}|\phi_1\sin\phi_1\right\}\right.\right.$$

$$\left.-\frac{3}{2}\left[\ln\left(\frac{\boldsymbol{l}_1^2}{\boldsymbol{k}^2}\right)+\ln\left(\frac{(\boldsymbol{l}_1-\boldsymbol{k})^2}{\boldsymbol{k}^2}\right)\right]-\ln\left(\frac{\boldsymbol{l}_1^2}{\boldsymbol{k}^2}\right)\ln\left(\frac{(\boldsymbol{l}_1-\boldsymbol{k})^2}{s_0}\right)-\ln\left(\frac{(\boldsymbol{l}_1-\boldsymbol{k})^2}{\boldsymbol{k}^2}\right)\ln\left(\frac{\boldsymbol{l}_1^2}{s_0}\right)-2\phi_1^2+\{1\leftrightarrow 2\}\right\}+2\pi^2+\frac{14}{3}\Big]$$

$$+\int_{z_0}^1 dz\left\{\ln\frac{\lambda^2}{\mu_F^2}S_J^{(2)}(\boldsymbol{k},zx)\left[P_{qq}(z)+\frac{C_a^2}{C_f^2}P_{gq}(z)\right]+\left[(1-z)\left[1-\frac{2}{z}\frac{C_a^2}{C_f^2}\right]+2(1+z^2)\left(\frac{\ln(1-z)}{1-z}\right)_+\right]S_J^{(2)}(\boldsymbol{k},zx)+4S_J^{(2)}(\boldsymbol{k},x)\right\}$$

$$+\int_0^1 dz\int\frac{d^2\boldsymbol{q}}{\pi}\left[P_{qq}(z)\Theta\left(\hat{M}_{X,\max}^2-\frac{(\boldsymbol{p}-z\boldsymbol{k})^2}{z(1-z)}\right)\Theta\left(\frac{|\boldsymbol{q}|}{1-z}-\lambda\right)\right.$$

$$\times\frac{\boldsymbol{k}^2}{\boldsymbol{q}^2(\boldsymbol{p}-z\boldsymbol{k})^2}S_J^{(3)}(\boldsymbol{p},\boldsymbol{q},(1-z)x,x)+\Theta\left(\hat{M}_{X,\max}^2-\frac{\boldsymbol{\Delta}^2}{z(1-z)}\right)S_J^{(3)}(\boldsymbol{p},\boldsymbol{q},zx,x)P_{gq}(z)$$

$$\left.\left.\times\left\{\frac{C_a}{C_f}[J_1(\boldsymbol{q},\boldsymbol{k},\boldsymbol{l}_1,z)+J_1(\boldsymbol{q},\boldsymbol{k},\boldsymbol{l}_2,z)]+\frac{C_a^2}{C_f^2}J_2(\boldsymbol{q},\boldsymbol{k},\boldsymbol{l}_1,\boldsymbol{l}_2)\Theta(\boldsymbol{p}^2-\lambda^2)\right\}\right]\right]$$

Conclusions

Conclusions

- Single Pomeron exchange is still an exciting exploration ground.
- Success in both perturbative and non-perturbative approaches
- Mueller Navelet Jets have been difficult to extract BFKL effects from, but new observables might pave the way forward
- Mueller Tang Jets show clear BFKL effects so far, but improved results can be computed with improved numerical analysis

Collaborators: Federico Deganutti, David Gordo Gomez, Christophe Royon, Chung-I Tan, Richard Brower, Richard Nally, Miguel Costa, Marko Djuric

Outreach

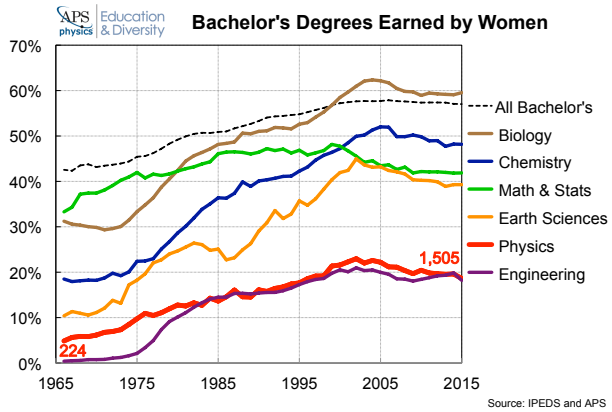

Why are we last!?

NSF

GK-12
www.gk12.org/

Get out and teach!

More Plots: Central Production

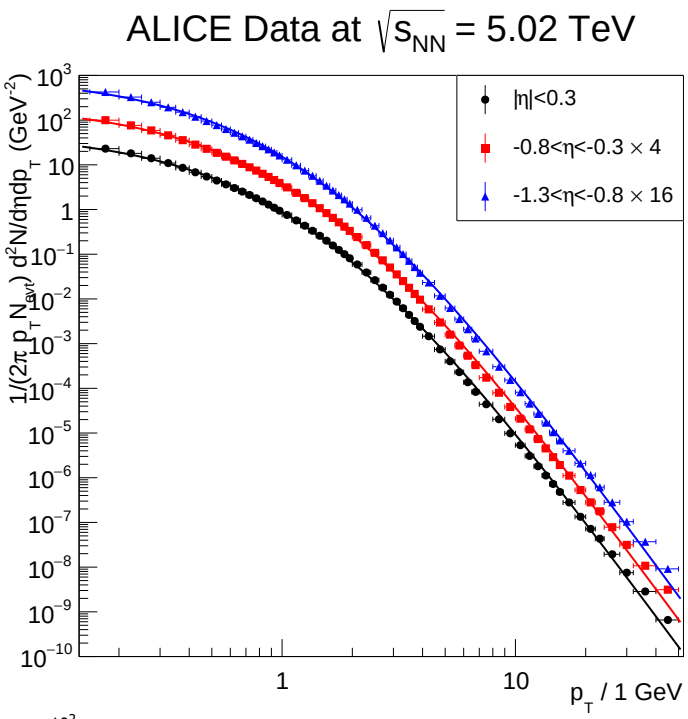

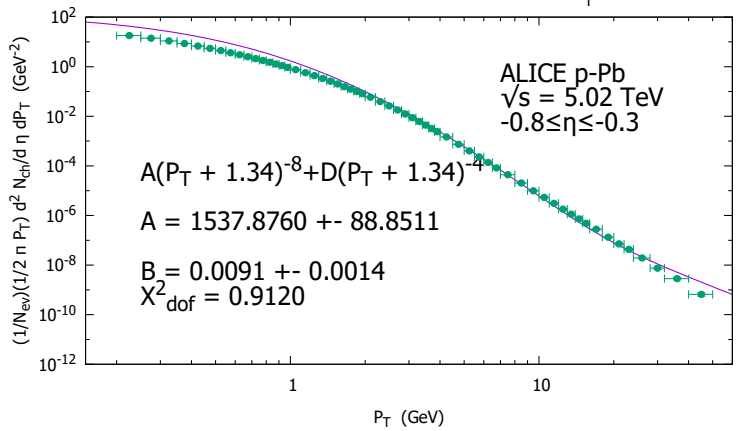

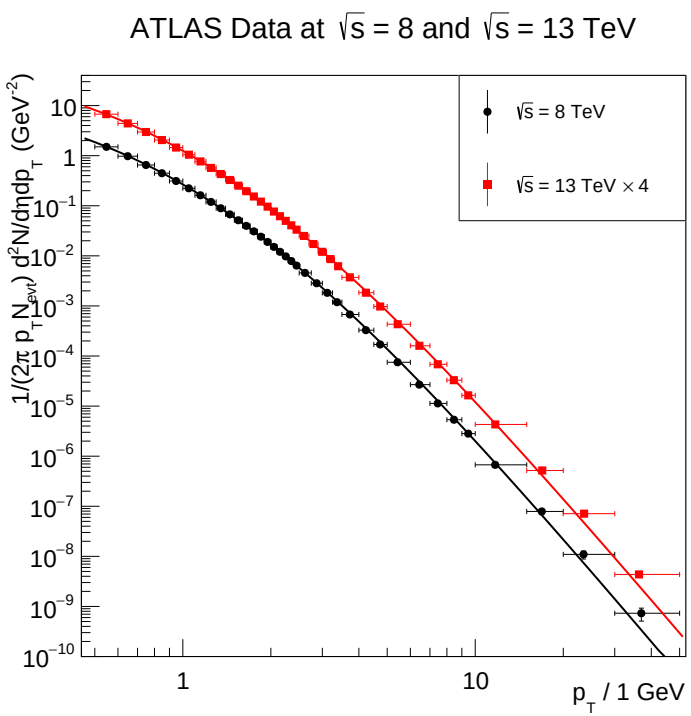

For $d\sigma \sim A/(P_T + C)^B$
$B \sim 7,\ C \sim 1\text{GeV}$
This is above Λ_{QCD}, small p_T behavior might be different. Not exactly the expected p_T^{-8} behavior expected! Still, $\chi^2_{dof} \sim 1$

More Plots: Saturation in DIS

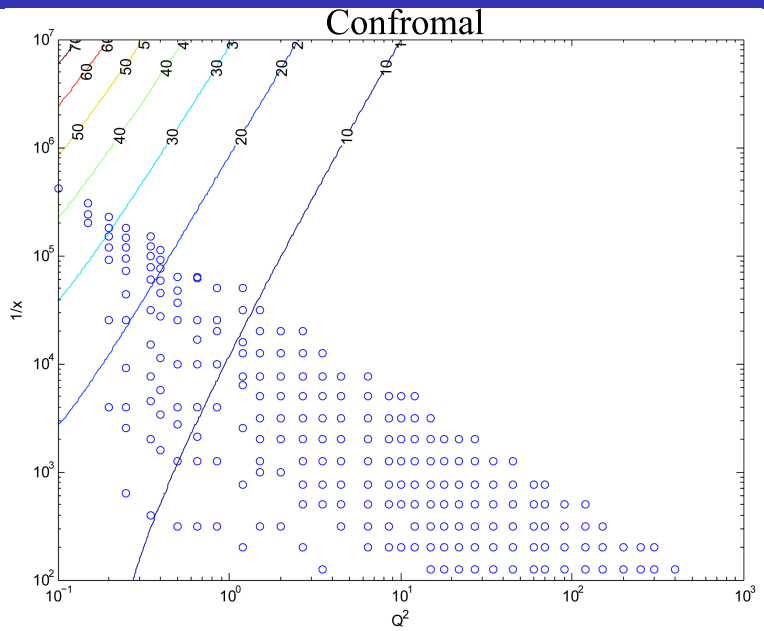

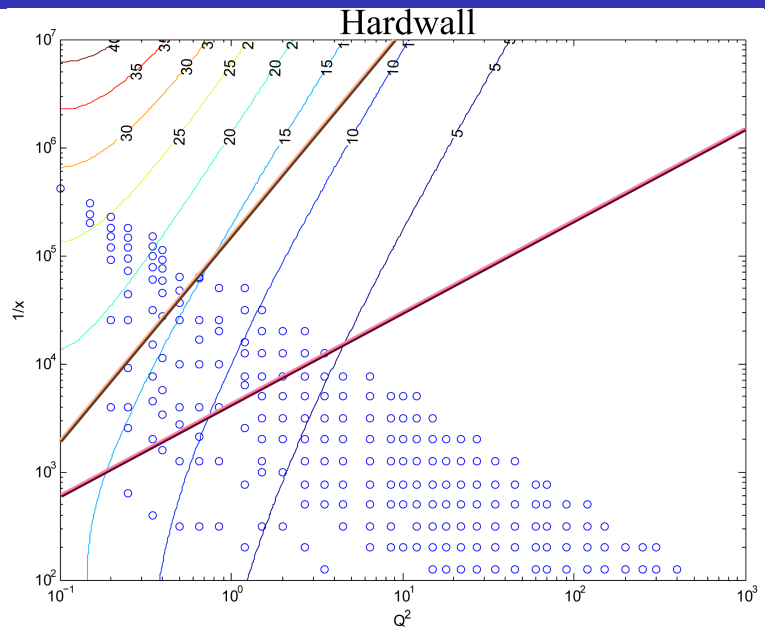

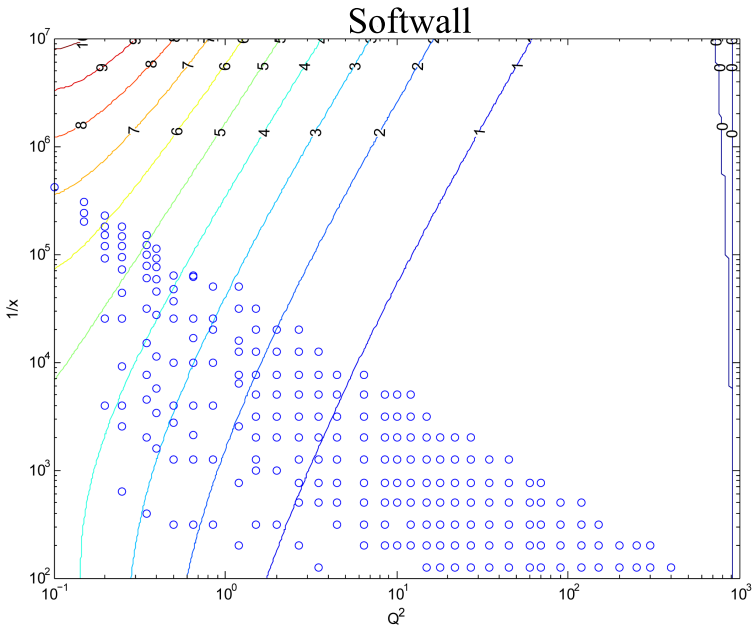

Contour plots of $\mathrm{Im}[\chi]$ as a function of $1/x$ vs Q^2 (Gev) for conformal, hard-wall, and softwall models. These plots are all in the forward limit, but the impact parameter representation can tell us about the onset of non-linear eikonal effects. The similar behavior for the softwall implies a similar conclusion about confinement vs saturation.

Nice Features of BPST Pomeron

- Λ controls the strength of the soft wall and in the limit $\Lambda \to 0$ one recovers the conformal solution

$$\mathrm{Im}\chi_P^{conformal}(t=0) = \frac{g_0^2}{16}\sqrt{\frac{\rho^3}{\pi}}(zz')\frac{e^{(1-\rho)\tau}}{\tau^{1/2}} exp\left(\frac{-(\mathrm{Log}z - \mathrm{Log}z')^2}{\rho\tau}\right)$$

where $\tau = \mathrm{Log}(\rho zz's/2)$ and $\rho = 2 - j_0$. Note: this has a similar behavior to the weak coupling BFKL solution where

$$\mathrm{Im}\chi(p_\perp, p'_\perp, s) \sim \frac{s^{j_0}}{\sqrt{\pi \mathcal{D}\mathrm{Log}s}}\exp(-(\mathrm{Log}p'_\perp - \mathrm{Log}p_\perp)^2/\mathcal{D}\mathrm{Log}s)$$

- If we look at the energy dependence of the pomeron propagator, we can see a softened behavior in the forward regge limit.

$$\chi_{conformal} \sim -s^{\alpha_0}\mathrm{Log}^{-1/2}(s) \to \chi_{HW} \sim -s^{\alpha_0}/\mathrm{Log}^{-3/2}(s)$$

Analytically, this corresponded to the softening of a j-plane singularity from $1/\sqrt{j - j_0} \to \sqrt{j - j_0}$. Again, we see this same softened behavior in the soft wall model.

- (Possibly) interesting limit: conformal quantum mechanics. Here the EOM simplifies and takes the form of a model with 1+1 dimensional conformal symmetry[Fubini]

LL BFKL

BFKL Eigenfunctions

$$\tilde{E}_{n\nu}(k_1, k_2) = N(n,\nu)\left[k_1^{*\,\bar{h}-2} k_2^{*\,h-2}\ {}_2F_1(1-h, 2-h; 2, -\frac{k_1}{k_2})\ {}_2F_1(1-\bar{h}, 2-\bar{h}; 2, -\frac{k_2^{*}}{k_1^{*}}) + \{1 \to 2\}\right]$$

where $h = \left(\frac{n+1}{2} + i\nu\right), \quad \bar{h} = \left(\frac{n-1}{2} - i\nu\right)$

At LL accuracy the Gluon green function G resumms to all orders of perturbation theory the ladder diagrams composed by s-channel gluons connected to t-channel reggeizzed gluons through the Lipatov vertex.

The normalization of the Gluon Green function fixes the jet vertex leading order.

$$\lim_{Y\to 0} G(\mathbf{k}, \mathbf{k}', \mathbf{q}, Y) = G(\mathbf{k}, \mathbf{k}', \mathbf{q}, 0) = \frac{\delta^2(\mathbf{k}-\mathbf{k}')}{\mathbf{k}^2(\mathbf{q}-\mathbf{k})^2}.$$

At this order, apart for the jet distribution function S that fixes the jet momentum, the jet vertex is a simple color factors (c-number)

$$V_a(x, \mathbf{q}, x_J, \mathbf{k}_J) = S_J^0(x, \mathbf{q}; x_J, \mathbf{k}_J) h_a^0,$$

$$h_a^0 = C_{q/g}^2 \frac{\alpha_s^2}{N_c^2 - 1}, \qquad S_J^{(0)} = x\delta^2(\mathbf{k}_J - \mathbf{q})\delta(x_J - x).$$

The independence of the LO vertices from the reggeon momenta allow for considerable simplification.

NLO impact factors

In general the cross section for these processes is given as a multiple convolution between the the jet vertices and the GGFs.

$$\frac{d\hat{\sigma}}{d\mathcal{J}_1 d\mathcal{J}_2 d^2\mathbf{q}} = \int d^2\mathbf{k}_1 d^2\mathbf{k}'_1 d^2\mathbf{k}_2 d^2\mathbf{k}'_2 V_a(\mathbf{k}_1, \mathbf{k}_2, \mathcal{J}_1, \mathbf{q}) \times$$
$$G(\mathbf{k}_1, \mathbf{k}'_1, \mathbf{q}, Y) G(\mathbf{k}_2, \mathbf{k}'_2, \mathbf{q}, Y) V_b(\mathbf{k}'_1, \mathbf{k}'_2, \mathcal{J}_2, \mathbf{q}), \qquad \mathcal{J} = \{\mathbf{k}_\mathcal{J}, x_\mathcal{J}\}.$$

Jet Functions for NLO impact factor

$$J_1(q, k, l, z) = \frac{1}{2}\frac{k^2}{(q-k)^2}\left(\frac{(1-z)^2}{(q-zk)^2} - \frac{1}{q^2}\right) - \frac{1}{4}\frac{1}{(q-l)^2}\left(\frac{(l-z\cdot k)^2}{(q-zk)^2} - \frac{l^2}{q^2}\right)$$
$$- \frac{1}{4}\frac{1}{(q-k+l)^2}\left(\frac{(l-(1-z)k)^2}{(q-zk)^2} - \frac{(l-k)^2}{q^2}\right);$$

$$J_2(q, k, l_1, l_2) = \frac{1}{4}\Bigg[\frac{l_1^2}{(q-k)^2(q-k+l_1)^2} + \frac{(k-l_1)^2}{(q-k)^2(q-l_1)^2}$$
$$+ \frac{l_2^2}{(q-k)^2(q-k+l_2)^2} + \frac{(k-l_2)^2}{(q-k)^2(q-l_2)^2} - \frac{1}{2}\Bigg(\frac{(l_1-l_2)^2}{(q-l_1)^2(q-l_2)^2}$$
$$+ \frac{(k-l_1-l_2)^2}{(q-k+l_1)^2(q-l_2)^2} + \frac{(k-l_1-l_2)^2}{(q-k+l_2)^2(q-l_1)^2} + \frac{(l_1-l_2)^2}{(q-k+l_1)^2(q-k+l_2)^2}\Bigg)\Bigg].$$